A method for identifying Sound Scattering Layers and extracting key characteristics

Scattering Layer identification and description

Word count: ~7650

Roland Proud[1,2,3], Martin J. Cox[2]; Simon Wotherspoon[3] and Andrew S. Brierley[1]

[1]Pelagic Ecology Research Group, Scottish Oceans Institute, University of St Andrews; [2]Australian Antarctic Division; [3]Institute of Marine and Antarctic Studies, University of Tasmania

Corresponding author:

Mr Roland Proud

University of St Andrews

Pelagic Ecology Research Group

Gatty Marine Laboratory

Scottish Oceans Institute

School of Biology

St Andrews

KY16 8LB Scotland

email: rp43@st-andrews.ac.uk

Abstract

1. Mid-trophic level water-column (pelagic) marine communities comprise millions of tonnes of zooplankton and micronekton that form dense and geographically-extensive layers, known as Sound Scattering Layers (SSLs) when observed acoustically. SSLs are ubiquitous in the global ocean and individual layers can span entire ocean basins. Many SSLs exhibit clear diel vertical migration behaviour. Vertical migrations contribute substantially to the 'biological pump', such that SSLs have important global biogeochemical roles: SSLs are important conduits for vertical energy and nutrient flow. Ship-based remote sensing of SSLs using acoustic instruments (echosounders) enables their shape and density to be quantified, but despite SSLs being discovered in the 1940s, there is no consistent method for identifying or characterizing SSLs. This hampers ecological and biogeographical studies of SSLs.

2. We have developed an automated and reproducible method for SSL identification and characterization, the Sound Scattering Layer Extraction Method (SSLEM). It functions independently of echosounder frequency and the spatial scale (vertical and horizontal) of the data. Here we demonstrate the SSLEM through its application to identify SSLs in data gathered to a depth of 1000 m using 38 kHz hull-mounted echosounders in the South West Indian Ocean and Tasman Sea.

3. SSLs were identified in the water-column as horizontally extensive echoes that were above background noise. For each identified SSL a set of 9 quantitative 'SSL metrics' (describing their shape, dynamics and acoustic backscattering

distribution) were determined, enabling inferences to be made concerning the spatial arrangement, distribution and heterogeneity of the biological community. The method was validated by comparing its output to a set of visually-derived SSL metrics that were evaluated independently by 8 students. The SSLEM outperformed the by-eye analysis, identifying three times the number of SSLs and with greater validity; 95% of SSLs identified by the SSLEM were deemed valid, compared to 75% by the students.

4. In the same way that data obtained from satellites has enabled the study and characterization of global phytoplankton distribution and production, we envisage that the SSLEM will facilitate robust, repeatable and quantitative analysis of the growing body of SSL observations arising from underway acoustic observations, enhancing our understanding of global ocean function.

Key-words:
Sound Scattering Layer Extraction Method; SSLEM; Deep Scattering Layers; biological layers; marine acoustics; SSL metrics; mid-trophic level; pelagic ecology; biological communities; diel vertical migration

Introduction

Sound Scattering Layers (SSLs) or Deep Scattering Layers (DSLs) are vertically discrete (100s of m or less) water column aggregations of organisms that can extend horizontally over 1000s of km (Kloser et al. 2009). The layers are comprised of pelagic organisms (organisms of the water column, as opposed to benthic organisms that live on or in the seabed), primarily zooplankton and small fish (cm to 10s cm), living together in distinct communities. When insonified, these organisms produce a distinct echo that, depending upon depth and incident acoustic frequency, can stand out prominently as scattering layers above background noise (Simmonds & MacLennan 2005). Such layers have been known since the mid 20th century when naval sonars detected signals thought initially to be echoes from the sea bed: the depths of the echoes however changed with time of day and it became apparent that these 'false bottoms' were in fact biological in origin (Brierley 2014).

The organisms that comprise SSLs are responsible for the transport of vast quantities of carbon (increasing particle export by up to 40% - Bianchi 2013) from the surface to the deep sea (the biological pump) via Diel Vertical Migration (DVM), the largest known daily migration of biomass on the planet (Hays 2003). They thus play an important role in atmosphere-ocean interactions, and in the global biogeochemical cycle. SSL scales can vary from the micro, at vertical resolutions of centimetres over timescales of a fraction of a minute (Holliday et al. 2003; McManus et al. 2003, 2005) to pan-oceanic (Anderson, Brierley, & Armstrong 2004; Kloser et al. 2009; Irigoien et al. 2014). The former, so called 'microlayers' provide an explanation for the 'paradox of the plankton' where high species diversity occurs in what at first glance may appear to be a homogenous volume

100 of water. Vertical structure means that the water column is in fact far from
101 homogenous. Its physical properties can change dramatically over just a few cm's or
102 meters enabling the discrete formation of aggregates at specific depth ranges
103 (Longhurst 1998). In this way, SSLs show the water column divided into multiple
104 vertically discrete habitats. Despite the importance of SSLs to ocean and earth-system
105 function, there is no accepted standard method for identifying or classifying them. This
106 in turn has hampered comparative or integrative studies of SSLs.
107
108 There are parallels between the pelagic and tropical rain forest ecosystems, in as far as
109 both have vertical (depth) layered structure that with increasing depth is increasingly
110 light-limited. The sea surface, like the forest canopy, can be studied remotely by
111 satellites and yield estimates of biomass and primary production (PP) (Longhurst,
112 2003; Anderson, 2012). The sea bed is a physically-fixed entity and organisms living
113 there, like organisms and vegetation of the forest floor, are amenable to study because
114 they are constrained by a two dimensional environment. The ocean interior, however, is
115 physically dynamic, and its inhabitants – pelagic organisms including zooplankton and
116 fish – have freedom to move in three dimensions so the dynamics of the sometimes-
117 dense layers of mid-trophic level communities are poorly understood (Lehodey,
118 Murtugudde & Senina, 2010) . Developments in forest sampling can perhaps guide
119 developments in ocean sampling.
120
121 In an effort to improve understanding of rainforest interiors, the 'RAINFOR' project
122 (Malhi et al., 2002) that was established over a decade ago initialised a network of
123 sampling sites for Amazonian rainforest ecosystems. As part of the initiative, field
124 measurements of the forest interior were taken and the data related back to satellite

information in order to gain a more complete picture of the ecosystem and to provide the capability to validate remotely-sensed data. Since the rainforest covers less than 7% of the earth's surface (Bierregaard et al., 1992; Wilson, 1994), a network of sites can provide a representative sample. The ocean on the other hand, covers over 71% of the earth's surface and therefore makes it extremely difficult, logistically and financially to study the pelagic community by insitu biological sampling alone. The required greater spatial coverage for the ocean can be achieved by using active acoustic sampling techniques (scientific echosounding) to rapidly observe large volumes of the ocean, from ship-based instruments routinely used on both research and fishing vessels. These acoustic data can help reveal the spatial structure of pelagic communities: many marine organisms scatter sound waves in a characteristic fashion (dependant on the frequency of the incident wave and anatomy of the organism) such that 'remote sensing' by echosounder can provide community insight. These data could then be linked back to remotely sensed PP data at the surface, acquired from online resources such as the National Oceanographic Data Centre (NODC, www.nodc.noaa.gov) and validated by biological point samples, available from, for example, the Ocean Biogeographical Information System (OBIS, www.iobis.org). Acoustic survey data already exist in vast quantities, with wide geographic coverage, leading to the possibility that a method capable of identifying and characterising pelagic communities, found within SSLs, would, akin to the RAINFOR project, potentially enable deep ocean processes to be inferred from satellite observation of the surface, yielding a more complete understanding of ocean ecosystem function. To achieve this, first a repeatable technique to identify and parameterise SSLs is required.

Some quantitative research has already been carried out on SSLs. Regional structure of SSLs has been identified by comparing total water-column backscattering strength at sites across the Pacific and Atlantic Oceans, in the Caribbean, Labrador, Norwegian and Mediterranean Seas and in Baffin Bay (Chapman et al. 1974) and also in the Atlantic and North Western Pacific using depth-frequency structure of backscattering strength (Andreeva, Galybin, & Tarasov 2000; Tarasov 2002). Biomass estimates of SSLs have also been made at the basin scale using both echo counting and echo integration techniques, in the Tasman Sea for example (Kloser et al. 2009). More recently, a method was developed to extract SSLs (Cade and Benoit-Bird 2014), that required input parameters such as an acoustic threshold intensity and minimum separation distances between SSLs to be defined a priori.

Research on SSLs has, however, typically been qualitative. The depth structure of SSLs has been observed to vary over large spatial scales in both longitude and latitude (Kloser et al. 2009), across ocean basins (Anderson, Brierley, & Armstrong 2004) in the Irminger Sea and across fronts (Nicol et al. 2000; Kawaguchi et al. 2010) in the Southern Ocean. Studies at oceanic features have also shown characteristic behaviour, such as bulges in SSLs at continental shelves (Jarvis et al. 2010) off East Antarctica and bowl-like SSL features forming under eddy structures (Godø et al. 2012) in the Norwegian Sea.

Conversely, discrete, biological aggregations - schools, shoals and swarms - have been quantitatively defined. The fisheries acoustic community has wrestled for years over the question of what, as seen in an acoustic record, is a school, and some standard identification and description protocols have been agreed (Reid and Simmonds 1993;

175 Reid 2000). The importance of particular school metrics for school identification has
176 differed between studies; for example Coetzee (2000), using the Shoal Analysis and
177 Patch estimation system algorithm (SHAPES: Barange 1994), identified morphological
178 aspects to be the chief descriptor; Lawson (2001), identified school energetics and
179 water-column position as the most important parameters.
180
181 In spite of previous work, no standardised objective approach exists for defining SSLs,
182 rendering comparisons between studies and between water-column communities and
183 the environment difficult beyond the merely descriptive. The lack of a consistent
184 analytical approach was identified by Handegard et al. (2013) as hindering marine
185 ecosystem monitoring and management.
186
187 Our overarching goal was to develop a standardised analysis method to extract
188 biological layers consistently from underway-acoustic survey data. We illustrate the
189 utility of our method here by identifying SSLs from data observed at 38 kHz in the South
190 West Indian Ocean and Tasman Sea. Application of this method will lead to a better
191 understanding of mid-trophic level communities, within and across oceanic boundaries
192 at varying spatial and temporal scales.
193
194
195
196
197
198
199

2 Materials and Method

2.1 Acoustic data

The acoustic data used in this study were all 38 kHz data and were obtained from the Integrated Marine Observing System data centre (IMOS, www.imos.au, downloaded on 1st June 2013). 38 kHz data were suitable for SSL observations because the moderately low attenuation rate (5 - 10 dB/km: Ainslie and McColm 1998) enables deep water-column penetration (up to 1500m) and because the wavelength is appropriate for detection of many of the fish and plankton species of the order of cm's that inhabit the layers. Data had been collected by research vessels (RV) *Southern Surveyor* and *Aurora Australis*, as well as several fishing vessels (FVs) including the *Southern Champion*, *Janas*, *Rehua*, *Austral Leader II* and *Will Watch*. Data were granted by the Marine National Facility and processed by the Commonwealth Scientific and Industrial Research Organisation (CSIRO) Oceans and Atmosphere Flagship as part of the IMOS Bio-Acoustic Ships of Opportunity (BASOOP) Program. The data totalled 24 transects covering wide areas of the South West Indian Ocean and Tasman Sea (Fig. 1). Transect length ranged from 200 NM to 1800 NM and included 24hr (day/night) coverage across all seasons between 2009 and 2012. The spatial coverage of the tracks included 2 of the 4 major global ocean biomes as described by Longhurst (1998) - the Trades and Westerlies - and also spanned major frontal zones and boundaries including the Subtropical Convergence Zone (STCZ) and the Polar Front (PF).

225

226 [FIGURE 1]

227

228 We pre-processed IMOS data by removing dropped pings (a ping is a single acoustic
229 transmit/receive cycle; typical ping rate was 0.5 Hz) and noise spikes (caused for
230 example by violent ship's motion in rough seas), and partitioned data into separate
231 day/night segments, bounded by sunrise/sunset. In instances where, for example the
232 echosounder had been turned off for short periods, or the vertical sampling resolution
233 of the echosounder was changed, data were further segmented. An acoustic image, or
234 echogram, was created for each segment. The acoustic image was as a two-dimensional
235 array of backscatter values on a depth v time (or space) grid. Each cell in the image, an
236 acoustic pixel, had an associated timestamp, geographical position and depth. For each
237 image, echo intensity in the form of Mean Volume Backscattering Strength (MVBS -
238 Simmonds & MacLennan, 2005) was calculated at a cell resolution of 5m in depth (from
239 the surface down to 1000m) by 1 minute in time.

240

241 **2.2 SSL extraction method (SSLEM)**

242

243 Our objective was to provide a method that would function over the range of bio-
244 acoustical echosounder frequencies in common (and likely future) use, over horizontal
245 scales from bays to oceans, and on vertical scales that encompass microlayers (cm;
246 Holliday et al., 2003) upwards to tens and hundreds of m. The common observational
247 frequency band (18 to 200 kHz) spans the Rayleigh and geometric scattering regions for
248 most zooplankton and nekton. This means that small changes in frequency can result in
249 large changes in backscattering intensity and hence in SSL descriptors. Layers only

become apparent acoustically when they can be distinguished from background noise (sufficiently high signal-to-noise ratio – SNR). SNR is a function of organism packing density, acoustic Target Strength, depth, insonification frequency and power, and environmental conditions (Simmonds & MacLennan, 2005). SSL appearance may also be influenced by sampling resolution (Korneliussen et al., 2008): for transect data resolution is determined by ping rate, beam angle, depth and ship speed. The geographic scale of data is an important consideration as there are many oceanic processes that occur over different spatial and temporal scales, from micro-turbulence to decadal oscillations. A robust general method should be capable of resolving features of interest at the scale of the study being conducted, and for the organisms of interest in the environment in which they exist.

2.2.1 Identification of SSLs

The SSL extraction method (SSLEM) is based upon detection of a contrast in MVBS (Berge et al. 2014) between pixels within SSLs (relatively high MVBS signal) and background pixels outside (relatively low MVBS noise). For a simple SSL analysis, using a window of depth range Z and time/space extent X, one could identify a vertically 'static' SSL surrounded by empty water by selecting pixels for which MVBS intensities were greater than the mean, μ, over the entire window. Under such a scheme, for any acoustic pixel (px) within the analysis window,

$$\text{Equ. 1} \qquad ssl = \begin{cases} 1, & px > \mu \\ 0, & px \leq \mu \end{cases}$$

where *ssl* is a Boolean variable, taking a value of 1 for pixels that are deemed to belong to an SSL and 0 for those that are not. This simple process, useful as an introduction to

the method, assumes that the SSL is completely contained by the analysis window and the surroundings are made up of pixels with low MVBS that is attributable to background noise. This may not be the case; for example, a transition between depth intervals that exhibit a difference in background noise (inherently caused by time-varied gain (TVG) amplification of background noise) would yield a layer-like boundary of *ssl* pixels. To ensure that SSLs were surrounded by lower intensity MVBS (both towards the surface and the seabed), the depth interval of the analysis window was divided into two equal values, d_1 and d_2, and pixels were only deemed a SSL pixel (*ssl* value of 1) when their MVBS value was larger than both the MVBS means, μ_1 and μ_2, over each of the two regions of the split window (Fig. 2a), yielding a new equation for *ssl*:

$$\text{Equ. 2} \qquad ssl = \begin{cases} 1, & (px > \mu_1)\ AND\ (px > \mu_2) \\ 0, & otherwise \end{cases}$$

where μ_1 and μ_2, are calculated over the regions X by d_1 and X by d_2 respectively, and where d_1 is equal to d_2.

[FIGURE 2]

In practice, using a fixed analysis window does not capture all SSLs, since they are rarely vertically static: they may for instance oscillate with internal wave activity or migrate vertically. To accommodate this, an analysis column one pixel wide was used instead of a window. The column was moved pixel-by-pixel through the image evaluating the pixel at the centre of the column at each step, such that μ_1 and μ_2 were calculated over the specific column (single point in time-series), not the entire window, bounded either side of the central pixel by the depth ranges d_1 and d_2. For constant

values of d_1 and d_2 this approach would only work if all SSLs had the same thickness and were separated by distances larger than the size of d_1 or d_2: this is not the case. To overcome this problem the depth ranges d_1 and d_2, for each pixel evaluated, were varied in size from 2 pixels in height (this minimum, rather than 1, was used to avoid flooding the image with incorrectly assigned *ssl* pixels when analysing highly variable or 'noisy' images) up to the vertical extents of the image (Fig. 2b). Then, for any pixel within an image, evaluated using a dynamic column,

Equ. 3 $$ssl = \begin{cases} 1, & \left(\sum_{d_1=2}^{r-1} \sum_{d_2=2}^{R-r} (px > \mu_1) \; AND \; (px > \mu_2) \right) > 0 \\ 0, & otherwise \end{cases}$$

where r is equal to the row number of the pixel being evaluated and R equal to the total number of rows within the image; consequently, the first and last two rows of each image are not processed. Each pixel thus has multiple opportunities (for varying d_1 and d_2 values) to be attributed an SSL pixel. This ensured that both vertically static and migrant SSLs of varying thicknesses and separation distances would all be identified.

2.2.2 Phantom SSLs and SSL_{min}

On occasions when no SSL was present in the analysis column, pixels would sometimes erroneously be designated as SSL pixels as a result of the backscatter from individual or diffuse arrangements of organisms, tightly packed schools or swarms, variation of the physical properties of sea water, or by natural variation inherent within the data. The variable, SSL_{min}, which designated a fixed minimum horizontal extent for SSLs

(measured in space/time units), was therefore introduced to enable the identification of only those SSLs that were relevant to the scale of process being studied e.g. from ocean basin scale (large SSL_{min}) down to krill swarms (small SSL_{min}: Watkins et al. 1990). In spite of this precaution, the natural variation within the data still sometimes produced SSLs. These incorrectly identified SSLs, termed 'phantom SSLs' (Fig. 3) were removed in post processing (Section 3.1) by analysis of SSL signal-to-noise ratios; SSLs were removed where the mean SSL MVBS (signal) was smaller than the maximum background MVBS value (noise) by analysing the pixels immediately surrounding the layers.

[FIGURE 3]

2.2.3 Separation of merged SSLs

The SSL pixels identified in Section 2.2.1 were used to generate an SSL mask (Fig. 4b) that bounded pixels that were connected, termed SSL features. These features were not classified as SSLs at this point, as a single feature could consist of several merged SSLs. Features smaller than SSL_{min} were removed and internal gaps smaller than SSL_{min} within accepted features were filled (Fig. 4c).

[FIGURE 4]

Each feature was then segmented into individual SSLs which existed over a discrete depth range at each point along a time-series. This was achieved by implementing a region-based image segmentation process. A simple growing algorithm moved column by column through the image, initialising new regions (that would eventually grow into

346 individual SSLs) within features where SSLs merged or split (Fig. 5). SSLs identified in
347 this process that were smaller than SSL_{min} were ignored and not analysed further.
348
349 [FIGURE 5]
350
351 **2.2.4 Separation of vertically 'static' and migrant SSLs**
352
353 Vertically static SSLs were separated from upwardly or downwardly-migrating SSLs by
354 application of a Change Point Analysis (CPA: Page 1954). CPA can detect the existence of
355 multiple trends within a time series by analysing the cumulative deviation from the
356 mean over time. The CPA was conducted using a time-series of the mean depth change,
357 ΔZ, over a selected time interval, CPA_{int}, across each SSL (Fig. 6). The choice of CPA_{int} is
358 related to the size of SSL_{min}. For a relatively large value of SSL_{min} (> 4 hours for example)
359 a large CPA_{int} value can be chosen and will reduce the likelihood that undulating SSLs,
360 caused by internal waves, would be incorrectly segmented. For small values of SSL_{min}, a
361 CPA_{int} value should be selected to provide enough samples (>10) for the CPA to be
362 conducted appropriately. The deviation of ΔZ from its mean was calculated (Fig. 6b),
363 followed by the cumulative sum of this deviation (Fig. 6c), the most significant point of
364 change was indicated by the largest absolute value (Fig. 6c – black line), and quantified
365 by the range, CPA_{max}, of the cumulative sum values. A confidence interval (CI) was
366 calculated by determining the percentage of 1000 bootstrapped samples of ΔZ that
367 yielded a CPA_{max} value smaller than the original CPA_{max} value. Where a significant
368 change occurred (95% CI), indicating that a SSL changed from simply varying in depth
369 around a static mean to exhibit migrant behaviour (increasing/decreasing depth), SSLs
370 were separated into migrant and static components (Fig. 6).

[FIGURE 6]

The CPA was conducted iteratively, until no further statistically significant change (95% CI) within an image segment could be detected: this ensured that multiple migrations, during a diel cycle for example, would all be separated. Multiple migrations were unlikely to occur in this study since at an earlier stage we partitioned the data into separate day and night segments.

2.2.5 SSL metrics

For each individual SSL identified a set of SSL metrics were evaluated (Table 1). The depth, duration, MVBS, MVBS standard deviation, MVBS range and layer thickness described spatial extent and backscatter distribution. The vertical velocity and depth range were used to identify and describe migratory layers. The Background Noise Level (BNL) was used to quantify the maximum level of noise surrounding the SSL. The maximum value was taken to ensure that it would be greater than the mean MVBS value of SSLs consistent of natural variation within the data (phantom SSLs: Section 2.2.2).

[TABLE 1]

The SSL metrics were analysed (Section 3.2) to gain better insight into the nature of SSLs within the study region, enabling inferences concerning the pelagic community (spatial arrangement, distribution and heterogeneity) to be made.

396 **2.3 Validation framework**

397 In order to examine the efficacy of our automated SSL identification technique versus
398 the principal present approach, adopted by most acoustic-trawl surveys when assessing
399 fish stocks – visual scrutinisation (which may be subjective and prone to between-
400 operator inconsistencies) - we designed a validation framework to examine potential
401 differences between SSLs determined by the SSLEM and visually scrutinised acoustic
402 images. If visual scrutiny gave highly variable results, this would illustrate the difficulty
403 likely to be encountered in comparative studies and the requirement of an automated
404 method.

405

406 The validation was conducted using a subset of the IMOS data. Images from this subset
407 were published online at www.soundscatteringlayers.com. Independent visual scrutiny
408 was performed autonomously by a group of 8 students, all of whom had attended an
409 acoustic data collection and processing summer school
410 (www.depts.washington.edu/fhl/) and were either PhD candidates at the University of
411 St Andrews or the Florida International University. Each student estimated 3 SSL
412 metrics, namely the depth, MVBS and thickness for all SSLs they could identify that
413 persisted for a time period longer than 1 hour. Each student considered 10 images
414 selected randomly from a set of 50. The results of the visual scrutiny were compared to
415 those from SSLEM (see Results 3.1).

416

417 **3 Results:**

418 Sound Scattering Layers (SSLs) that persisted for time periods longer than 1 hour
419 (SSL_{min} = 60 minutes; CPA_{int} = 6 minutes: see Sections 2.2.2 and 2.2.4 respectively for
420 definitions) were identified and extracted from the IMOS dataset (Section 2.1) using the

SSL extraction method (SSLEM). SSLs were extracted at these setting in order to conduct a regional analysis of the study area, ensuring that only persistent and therefore characteristic SSLs were identified. In total, 2064 SSLs were extracted from 264 images that were on average 3.4 hours in length; an example of the identification of SSLs for an IMOS image is given in Fig. 4. 108 phantom SSLs (see Section 2.2.2) that were identified in the validation procedure were removed. For each SSL, SSL metrics described in Section 2.2.5 were determined and relationships found between select SSL metrics explored (Section 3.2).

3.1 SSLEM Validation

SSL Metrics that were estimated by the students from SSLs visually identified were mapped back on to the original acoustic images for comparison with the SSLEM identified SSLs. Each visually identified SSL was categorised as being a valid/invalid SSL identification. This process was mirrored using the output from the SSLEM, where phantom SSLs (see Section 2.2.2) were visually identified after extraction and deemed to be invalid SSLs comprised of background noise. The students identified 211 SSLs from 80 images. For the same SSLs that were identified by more than 6 of the students from the same image, mean ranges of the estimated metrics were calculated (Table 2).

[TABLE 2]

Of the three SSL identification fields in Table 2 (< SSL_{min}, Noise & TVG), the Time-Varied-Gain (TVG) field contained the largest proportion of the students misclassification of SSLs. The TVG increases the amplitude, as a function of time (or depth for a fixed sound speed) of the echo return and serves to amplify both signal, when organisms are present, and the background in an empty pixel, which appears in

446 the acoustic image as depth dependent noise (Simmonds & MacLennan, 2005). This
447 essentially limits the useful (range over which signal dominates noise) range of the
448 instrument and causes visible, layer-like bands to form at the far extent of this range.
449 These layers can resemble SSLs to the untrained eye, but not to the SSLEM; normally
450 TVG is removed in pre-processing but can just as easily be removed afterwards (e.g.
451 Watkins & Brierley, 1996).
452
453 The SSLEM identified, on average, over 3 times the number of SSLs per acoustic image
454 than the group of students. Whereas the SSLEM output included no variance between
455 repeat identifications and characterisations of SSLs from the same image, the overall
456 mean standard deviation of the number of SSLs identified per image for the students
457 was 0.54. This is in fact quite low, and demonstrates that although the students
458 identified fewer SSLs, the group broadly did agree on the number of SSLs per image.
459 Metric estimates by the students were, however, notably large, especially the mean
460 MVBS range (4.8 dB re $1m^{-1}$) that is equivalent to a factor 3 change in the linear domain.
461 The SSLs identified by the SSLEM were also much more likely to be valid (94.8%), i.e.
462 not phantom SSLs, than those identified by the students (only 75.4% valid), who
463 misidentified SSLs a quarter of the time (Table 2). The SSLEM extracted a total of 108
464 incorrect SSLs, all of which were considered to be phantom SSLs (Section 2.2.2).
465
466 Phantom SSLs form by the naturally occurring variation in the data. They are an artefact
467 of the SSLEM, and hence not detected by visual scrutinisation. This variability is of no
468 consequence within SSLs, but can cause false SSL identification outside (i.e. in empty
469 water - Fig. 3). In order to remove phantom SSLs, the Background Noise Level (BNL)
470 metric was used to identify SSLs that had low signal-to-noise ratios or more accurately,

low BNL-to-MVBS ratios. SSLs that had a MVBS value that was smaller than the BNL were identified as being phantom SSLs (black points in Fig. 7). Removing these SSLs from the results increased the validity of the automated method, for the data analysed in this study, to 100%.

[FIGURE 7]

Phantom SSLs are apparent throughout the entire water-column, except for the region between 400m and 800m. In this depth region within the study location of the South West Indian Ocean and Tasman Sea, strong and broad SSLs were persistently present (Fig. 8), meaning that SSLs dominated, excluding the possibility of phantom SSLs forming at the same depth.

3.2 SSL Metrics

The SSLEM output a total of 1956 valid (non-phantom) SSLs from the IMOS data. Each SSL was summarised by a set of 9 SSL metrics (Table 1).

[FIGURE 8]

Physical characteristics of SSLs provide biological/ecological insight into pelagic community dynamics. For example, the MVBS range increased towards the surface (Fig. 8a) suggesting that the biological community becomes more complex/heterogeneous in the epi-pelagic region; this could be caused by an increase in species diversity or a larger range of the orientations of organisms, caused by feeding for example. The broadest SSLs lie within the central portion of the mesopelagic region of the water-

column (Fig. 8b). The highest MVBS values (a proxy for increased biomass/abundance) occurred within the water-column at depths of around 600m and at the surface (Fig. 8c) and also geographically towards 40 degrees south (Fig. 8d). This is consistent with the fact that the zone is the highly productive Subtropical convergence zone (see Fig. 1; as identified by Longhurst 1998) where previous work has revealed an enhanced prey-field (Boersch-Supan et al. 2012).

4 Discussion:

4.1 Sound Scattering Layer Extraction Method (SSLEM)

The Sound Scattering Layer (SSL) Extraction Method (SSLEM) was demonstrated here using data observed at a single frequency, 38 kHz. However, the method is independent of frequency and is entirely appropriate for use with other frequencies. The main differences that would occur would be subject to the characteristics of the incident frequency, for example, reduced depth range and increased resolution at higher frequencies (Simmonds & MacLennan 2005).

The efficacy of the SSLEM was examined by comparing output from that of visually scrutinised data (Table 2). The comparison demonstrated that the SSLEM method is more effective at identifying SSLs (Section 3.1). Visually scrutinised images were subject to SSL misclassification, under classification and sample variation, whereas the SSLEM output was perfectly repeatable, with zero variance between repeat extractions of SSLs and metrics.

Merged vertically static and migrant SSLs were separated by an application of a change-point analysis (Section 2.2.4). Analysis of the derived SSL metrics revealed water-column and geographical trends (Fig. 8). Summarising these data into discrete metrics offers a method of standardised analysis for assessing variability in biological communities in the water-column. Importantly, acoustic survey data can now be condensed down from millions of values to a set of community descriptors that can be easily stored, shared and analysed.

4.2 SSLEM Applications

Analysis of the ocean's SSLs will enable the study of the ocean's mid-trophic structure, providing a global prey field that would be invaluable to predator-prey ecologists. SSL depths could be used to gauge energy expenditure of diving mammals (Boersch-Supan et al. 2012; Walters et al. 2014) and spatial arrangements of prey-fields that could be incorporated into existing biophysical models (for example, SEPODYM: Bertignac, Lehodey, & Hampton 1998; Lehodey et al. 1998). Monitoring the structure of SSLs over long time periods could reveal climatic influences and the knock-on effects for SSL inhabitants (Lehodey et al. 2003). Spatially distinct formations of SSLs made up of diverse communities are likely to be distinguished and characterized by SSL metrics, allowing the division of regionally distinct biological communities (Longhurst 1998). Whilst the SSLEM does not resolve communities at the species level, such as the Species Identification Methods from Acoustic Multifrequency Information (SIMFAMI: Gajate et al. 2004) project, the SSLEM offers an alternate and simpler approach for fisheries and conservation management regimes to assess and monitor open ocean ecosystem health and stability (Korneliussen et al. 2008; Handegard et al. 2013).

546

547 4.3 Summary

548

549 The SSLEM presented here is directly applicable to all acoustic images, including
550 echograms output from Acoustic Doppler Current Profilers (ADCPs), because it is
551 independent of frequency and scale. Furthermore, it naturally lends itself to more
552 complex multi-frequency analysis (Jarvis et al. 2010). Unlike other methods (e.g. Cade
553 and Benoit Bird, 2014), the SSLEM was built to facilitate automated processing of data
554 in a standardised fashion that would vary only with consideration of the resolution and
555 scale of the study in mind. It is our hope that its introduction will enable the analysis of
556 a wealth of data that is immediately available, offering insights into the biological
557 structure of the world's ocean. The derived SSL metrics provide a means to summarise
558 the extracted layers, making them readily available for a wide range of analysis.
559 Importantly, the SSLEM offers the opportunity to study the structure of the mid-trophic
560 communities in the ocean and will aid in improving our understanding of an ocean
561 ecosystem.

562

563 Acknowledgements:
564 We would like to give special thanks to the reviewers for some very helpful and
565 instructive comments. We would also like to acknowledge the help of the Integrated
566 Marine Observing System data centre (IMOS) and Rick Towler of NOAA for providing
567 vital code for the pre-processing of the acoustic data. Finally we would like to give
568 thanks to the students, namely Katie Kirk, Katie Wurtzell and Laura Hobbs whom
569 attended the Marine Bioacoustics workshop in Friday Harbor, Marta D'Elia from the
570 Florida International University and Sam Gordine, Mirko Semler, Chris Mueller & Moritz

Wiesel from the University of St Andrews, for taking the time to help with the validation of the method.

Data Accessibility:

Acoustic data are publicly available via the Integrated Marine Observing System (IMOS) - Bio-Acoustic Ships of Opportunity (BA SOOP) sub-facility found using the IMOS Ocean data portal: https://imos.aodn.org.au/imos123/home

References:

Ainslie, M.A., & McColm, J.G. (1998) A simplified formula for viscous and chemical absorption in seawater. *Journal of the Acoustical Society of America*, 103, 1671–1672.

Anderson, C.I.H., Brierley, A.S., & Armstrong, F. (2004) Spatio-temporal variability in the distribution of epi- and meso-pelagic acoustic backscatter in the Irminger Sea, North Atlantic, with implications for predation on *Calanus finmarchicus*. *Marine Biology*, 146(6), 1177–1188.

Andreeva, I.B., Galybin, N.N., & Tarasov, L.L. (2000) Vertical structure of the acoustic characteristics of deep scattering layers in the ocean. *Acoustical Physics*, 46(5), 505–510.

Brierley, A.S. (2014) Quick Guide: Diel Vetical Migration. *Current Biology*, 24(22), 1074 - 1076.

595 Barange, M., Hampton, I., Pillar, S.C., & Soule, M.A. (1994) Determination of composition
596 and vertical structure of fish communities using in situ measurements of acoustic target
597 strength. *Canadian Journal of Fisheries and Aquatic Sciences*, 51, 99–109.
598
599 Berge, J., Cottier, F., Varpe, Ø., Renaud, P. E., Falk-Petersen, S., Kwasniewski, S., Griffiths,
600 C., Søreide, J.E., Johnsen, G., Aubert, A., Bjaerke, O., Hovinen, J., Jung-Madsen, S., Tveit, M.
601 & Majaneva, S. (2014). Arctic complexity: a case study on diel vertical migration of
602 zooplankton. *Journal of plankton research*, 36(5), 1279-1297.
603
604 Bertignac, M., Lehodey, P., & Hampton, J. (1998). A spatial population dynamics
605 simulation model of tropical tunas using a habitat index based on environmental
606 parameters. *Fisheries Oceanography*, 7(3-4), 326-334.
607
608 Bianchi, D., Stock, C., Galbraith, E.D., & Sarmiento, J.L. (2013) Diel Vertical Migration:
609 Ecological controls and impacts on the biological pump in a one-dimensional ocean
610 model. *Global Biogeochemical Cycles*, 27, 478-491.
611
612 Bierregaard, R.O., Lovejoy, T.E., Kapos, V., dos Santos, A.A., & Hutchings, R.W. (1992) The
613 biological dynamics of tropical rainforest fragments. *BioScience*, 42, 859–866.
614
615 Boersch-Supan, P., Boehme, L., Read, J., Rogers, A., & Brierley, A. (2012) Elephant seal
616 foraging dives track prey distribution, not temperature: Comment on McIntyre et al.
617 (2011). *Marine Ecology Progress Series*, 461(4), 293–298.
618

619 Cade, D.E. & Benoit-Bird, K.J. (2014) An automatic and quantitative approach to the
620 detection and tracking of acoustic scattering layers (supplemental code). Oregon State
621 University Libraries. Software.
622
623 Chapman, R., Bluy, O., Adlington, R., & Robison, A. (1974) Deep scattering layer spectra
624 in the Atlantic and Pacific Oceans and adjacent seas. *The Journal of the Acoustical Society*
625 *of America*, 56(6), 1722–1734.
626
627 Coetzee, J. (2000) Use of a shoal analysis and patch estimation system (SHAPES) to
628 characterise sardine schools. *Aquatic Living Resources*, *13*(1), 1–10.
629
630 Gajate, J., Ponce, R., Peña, M., Iglesias, M., Fernandes, P., & Alvarez, F. (2004). The
631 SIMFAMI database: a library of ground truthed acoustic survey data. In *Annual Science*
632 *ICES Conference, ICES ASC*.
633
634 Godø, O.R., Samuelsen, A., Macaulay, G.J., Patel, R., Hjøllo, S.S., Horne, J., Kaartvedt, S. &
635 Johannessen, J.A. (2012) Mesoscale eddies are oases for higher trophic marine life. *PloS*
636 *One*, *7*(1), e30161.
637
638 Handegard, N.O., Buisson, L. du, Brehmer, P., Chalmers, S.J., Robertis, A., Huse, G., Kloser,
639 R., Macaulay, G., Maury, O., Ressler, P.H., Stenseth, N.C. & Godø, O.R. (2013) Towards an
640 acoustic-based coupled observation and modelling system for monitoring and
641 predicting ecosystem dynamics of the open ocean. *Fish and Fisheries*, 14(4), 605-615.
642

643 Hays, G. C. (2003) A review of the adaptive significance and ecosystem consequences of
644 zooplankton diel vertical migrations. *Hydrobiologia*, *503*(1-3), 163–170.
645
646 Holliday, D.V. & Donaghay, P.L., Greenlaw, C.F., Mcgehee, D.E., Mcmanus, M.M., Sullivan, J.
647 M., & Miksis, J.L. (2003) Advances in defining fine- and micro-scale pattern in marine
648 plankton. *Aquatic Living Resources*, 16, 131–136.
649
650 ICES WGTC: CRR 238 (2000) Editor: Dave Reid, Report on Echo Trace Classification.
651
652 IMOS (2013), IMOS BASOOP sub-facility, imos.org.au [accessed 1st June 2013].
653
654 Irigoien, X., Klevjer, T. A, Røstad, A., Martinez, U., Boyra, G., Acuña, J. L., Bode, A.,
655 Echevarria, F., Gonzalez-Gordillo, J. I., Hernandez-Leon, S., Agusti, S., Aksnes, D. L.,
656 Duarte, C. M. & Kaartvedt, S. (2014) Large mesopelagic fishes biomass and trophic
657 efficiency in the open ocean. *Nature Communications*, 5(May 2013), 3271.
658
659 Jarvis, T., Kelly, N., Kawaguchi, S., van Wijk, E., & Nicol, S. (2010) Acoustic
660 characterisation of the broad-scale distribution and abundance of Antarctic krill
661 (*Euphausia superba*) off East Antarctica (30-80°E) in January-March 2006. *Deep Sea*
662 *Research Part II: Topical Studies in Oceanography*, 57(9-10), 916–933.
663
664 Kawaguchi, S., Nicol, S., Virtue, P., Davenport, S.R., Casper, R., Swadling, K.M. & Hosie, G.
665 W. (2010) Krill demography and large-scale distribution in the Western Indian Ocean
666 sector of the Southern Ocean (CCAMLR Division 58.4.2) in Austral summer of 2006.
667 *Deep Sea Research Part II: Topical Studies in Oceanography*, 57(9-10), 934–947.

668

669 Kloser, R.J., Ryan, T.E., Young, J.W. & Lewis, M.E. (2009) Acoustic observations of
670 micronekton fish on the scale of an ocean basin : potential and challenges. *ICES Journal*
671 *of Marine Science*, 66, 998–1006.

672

673 Korneliussen, R.J., Diner, N., Ona, E., Berger, L. & Fernandes, P.G. (2008) Proposals for
674 the collection of multifrequency acoustic data. *ICES Journal of Marine Science*, 65, 982–
675 994.

676

677 Lawson, G. (2001) Species identification of pelagic fish schools on the South African
678 continental shelf using acoustic descriptors and ancillary information. *ICES Journal of*
679 *Marine Science*, 58(1), 275–287.

680

681 Lehodey, P., Andre, J. M., Bertignac, M., Hampton, J., Stoens, A., Menkès, C., Memery, L. &
682 Grima, N. (1998). Predicting skipjack tuna forage distributions in the equatorial Pacific
683 using a coupled dynamical bio-geochemical model. *Fisheries Oceanography*, 7(3-4), 317-
684 325.

685

686 Lehodey, P., Chai, F., & Hampton, J. (2003). Modelling climate-related variability of tuna
687 populations from a coupled ocean–biogeochemical-populations dynamics model.
688 *Fisheries Oceanography*, 12(4-5), 483-494.

689

690 Lehodey, P., Murtugudde, R. & Senina, I. (2010) Bridging the gap from ocean models to
691 population dynamics of large marine predators: a model of mid- trophic functional
692 groups. *Progress in Oceanography*, 84, 69–84.

693

694 Longhurst, A. (1998) Ecological Geography of the Sea, Academic Press, San Diego.

695

696 Malhi, Y., Phillips, O.L., Lloyd, J., Baker, T., Wright, J., Almeida, S., Arroyo, L., Frederiksen,
697 T., Grace, J., Higuchi, N., Killeen, T., Laurance, W.F., Leaño, C., Lewis, S., Meir, P.,
698 Monteagudo, A., Neill, D., Núñez Vargas, P., Panfil, S.N., Patiño, S., Pitman, N., Quesada,
699 C.A., Rudas-Ll, A., Salomão, R., Saleska, S., Silva, N., Silveira, M., Sombroek, W.G., Valencia,
700 R., Vásquez Martínez, R., Vieira, I.C.G. & Vinceti, B. (2002) An international network to
701 monitor the structure, composition and dynamics of Amazonian forests (RAINFOR).
702 *Journal of Vegetation Science,* 13(3), 439-450.

703

704 McManus, M.A., Alldredge, A.L., Barnard, A.H., Boss, E., Case, J.F., Cowles, T.J., Donaghay,
705 P.L., Eisner, L.B., Gifford, D.J., Greenlaw, C.F., Herren, C.M., Holliday, D.V., Johnson, D.,
706 MacIntyre, S., McGehee, D.M., Osborn, T.R., Perry, M.J., Pieper, R.E., Rines, J.E.B., Smith,
707 D.C., Sullivan, J.M., Talbot, M.K., Twardowski, M.S., Weidemann, A. & Zaneveld, J.R.
708 (2003) Characteristics, distribution and persistence of thin layers over a 48 hour period.
709 *Marine Ecology Progress Series*, 261, 1–19.

710

711 McManus, M., Cheriton, O., Drake, P., Holliday, D., Storlazzi, C., Donaghay, P. & Greenlaw,
712 C. (2005) Effects of physical processes on structure and transport of thin zooplankton
713 layers in the coastal ocean. *Marine Ecology Progress Series*, 301, 199–215.

714

715 Nicol, S., Pauly, T., Bindoff, N., Wright, S., Thiele, D., Hosie, G.W., Strutton, P.G. & Woehler,
716 E. (2000) Ocean circulation off east Antarctica affects ecosystem structure and sea-ice
717 extent. *Nature*, 406(August), 504–507.

718

719 Reid D.G. & Simmonds E.J. (1993) Image analysis techniques for the study of fish school
720 structure from acoustic survey data. *Canadian Journal of Fisheries and Aquatic Sciences*,
721 50, 886–893.

722

723 Simmonds, E.J. & MacLennan, D.N. (2005) Fisheries Acoustics: Theory and Practice, 2nd
724 edn. Blackwell Publishing, Oxford. 456 pp.

725

726 Stanton, T., Chu, D. & Wiebe, P. (1998) Sound Scattering by several zooplankton groups.
727 II. Scattering models. *The Journal of the Acoustical Society of America*, 103, 236-253.

728

729 Page, E.S. (1954) Continuous inspection schemes. *Biometrika*, 100-115.

730

731 Tarasov, L.L. (2002) Deep scattering layers in the northwestern pacific. *Acoustical*
732 *Physics*, 48(1), 81–86.

733

734 Walters, A., Lea, M.A., van den Hoff, J., Field, I.C., Virtue, P., Sokolov, S., Pinkerton, M.H. &
735 Hindell, M.A. (2014) Spatially Explicit Estimates of Prey Consumption Reveal a New Krill
736 Predator in the Southern Ocean. *PloS one*, *9*(1), e86452.

737

738 Watkins, J.L., Morris, D.J., Ricketts, C. & Murray, A.W.A. (1990) Sampling biological
739 characteristics of krill: effect of heterogeneous nature of swarms. *Marine Biology*, 107,
740 409-415.

741

742 Watkins, J.L. & Brierley, A.S. (1996) A post-processing technique to remove background
743 noise from echo integration data. *ICES journal of Marine Science*, 53, 339-344.
744
745 Wilson, E.O. (1994) Biodiversity: Challenge, science, opportunity. *American Zoologist*,
746 34, 5–11.
747
748
749
750
751
752
753
754
755
756
757
758
759
760
761
762
763
764
765
766

SSL metric	Definition	Unit
Depth	mean depth	m
Depth range	Max(depth) – Min(depth)	m
MVBS	MVBS over entire SSL	dB re $1m^{-1}$
MVBS range	Max(MVBS) - Min(MVBS)	dB re $1m^{-1}$
MVBS STD	standard deviation of MVBS	dB re $1m^{-1}$
Thickness	mean SSL thickness	m
Vertical velocity	(change in depth)/time	ms^{-1}
Background Noise Level (BNL)	Max (MVBS) of background pixels surrounding SSL	dB re $1m^{-1}$
Duration	length of SSL duration	(H:M:S)

Table 1 – Sound Scattering Layer (SSL) metrics: summary metrics for individual SSLs. The unit dB re $1m^{-1}$ represents 10 times the log base 10 value of a variable with units of m^{-1}, in this case the mean volume backscattering coefficient (Simmonds & MacLennan, 2005), that is relative to a reference level of $1m^{-1}$.

Method	Mean depth range (m)	Mean MVBS range (dB re $1m^{-1}$)	Mean thickness range (m)	< SSL_{min} (%)	Noise (%)	TVG (%)	Valid (%)	Invalid (%)
SSLEM	0	0	0	0	5.2	0	94.8	5.2
VISUAL	26.3	4.8	53	5.7	8.5	10.4	75.4	24.6

Table 2 – Summary of method output versus visual scrutiny for identification of Sound Scattering Layers (SSLs). Columns definitions from left to right: Method – method of SSL identification; Mean depth range, Mean MVBS range & Mean thickness range – mean ranges of values for the depth, MVBS and thickness metrics for repeat estimations of the same SSLs; < SSL_{min} – percentage of SSLs identified smaller than the pre-set minimum value; Noise – percentage of SSLs consistent of background noise (including phantom SSLs); TVG – percentage of SSLs made up of 'layer-like' noise bands amplified by time-varied gain (TVG); Valid – number of correctly identified SSLs; Invalid – number of incorrectly identified SSLs. Percentages and means are to 1 d.p.

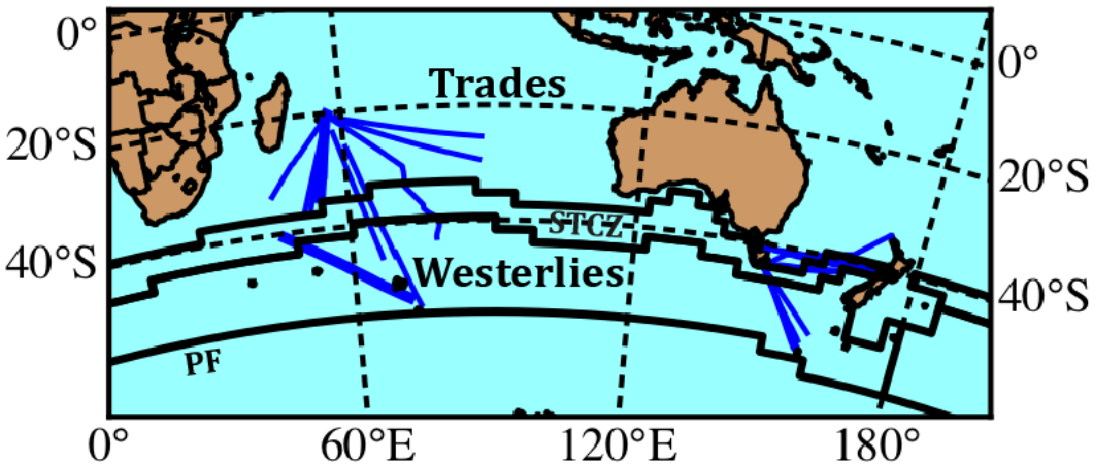

Figure 1 - Map showing ship transect lines (blue) for acoustic data extracted from the Integrated Marine Observing System (IMOS) data centre. Mean positions of the Subtropical Convergence Zone (STCZ) and Polar Front (PF) are marked as well as two Longhurst Biomes, the Trades and the Westerlies, separated by the northern boundary of the STCZ.

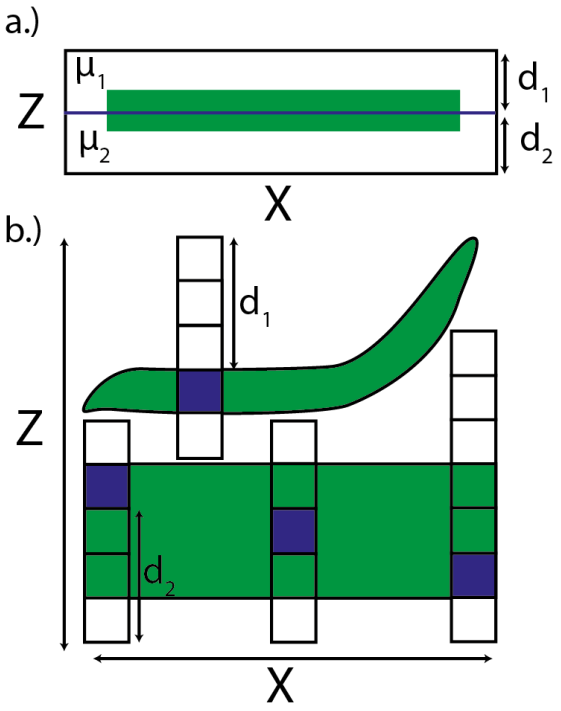

Figure 2 - Identification of Sound Scattering Layer (SSL) pixels, where green features indicate relatively high intensity SSLs, white background indicates low intensity noise (or empty water) and blue cells represent the SSL pixel being evaluated. a.) Simple SSL analysis window: only vertically static SSLs separated by a distance larger than d_1 or d_2 are detected b.) Dynamic SSL analysis column: a column is moved pixel by pixel through the image, where at each step the column size ranges from the minimum (5 pixels in length; where d_1 and d_2 are both equal to 2 pixels plus the pixel being evaluated) up to the full vertical extent of the Z axis, by stepping through all the possible values for each of the two parameters, d_1 and d_2; in doing so, SSLs of varying separation distances and vertical behaviours are captured.

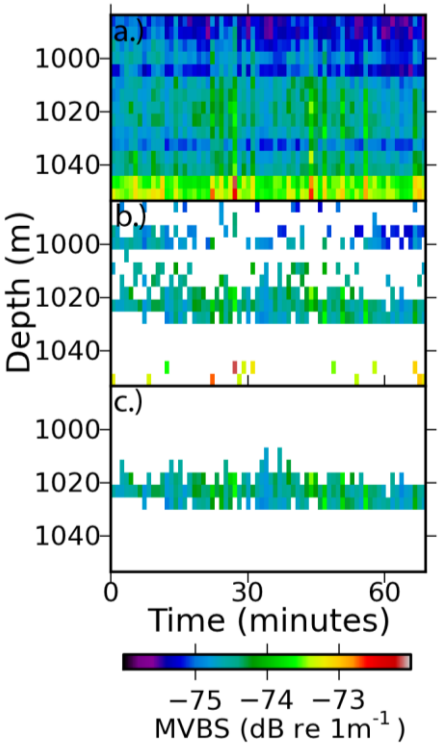

Figure 3 – Phantom Sound Scattering Layer (SSL) extracted from FV *Austral Leader II* transect during May 2012, where SSL_{min}, the minimum horizontal resolution of SSLs, was set to 60 minutes a.) acoustic image segement; b.) SSL pixels identified by the method (Section 2.2.1). c.) Extracted phantom SSL: MVBS values of the SSL are similar to that of the surrounding background.

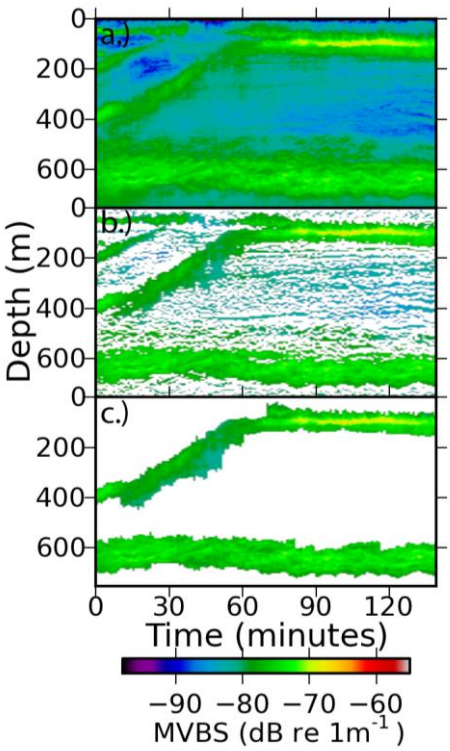

Figure 4 - Processed acoustic image, from FV *Austral Leader II* transect during May 2012, where SSL_{min}, the minimum horizontal resolution of Sound Scattering Layers (SSLs), was set to 60 minutes. a.) Original acoustic image at a resolution of 5m in depth and 1 minute in time. b.) Masked image: only pixels that are deemed to be potential SSL pixels are shown. c.) SSLs identified after removing features smaller than SSL_{min} and filling SSL internal gaps (that are smaller than SSL_{min}).

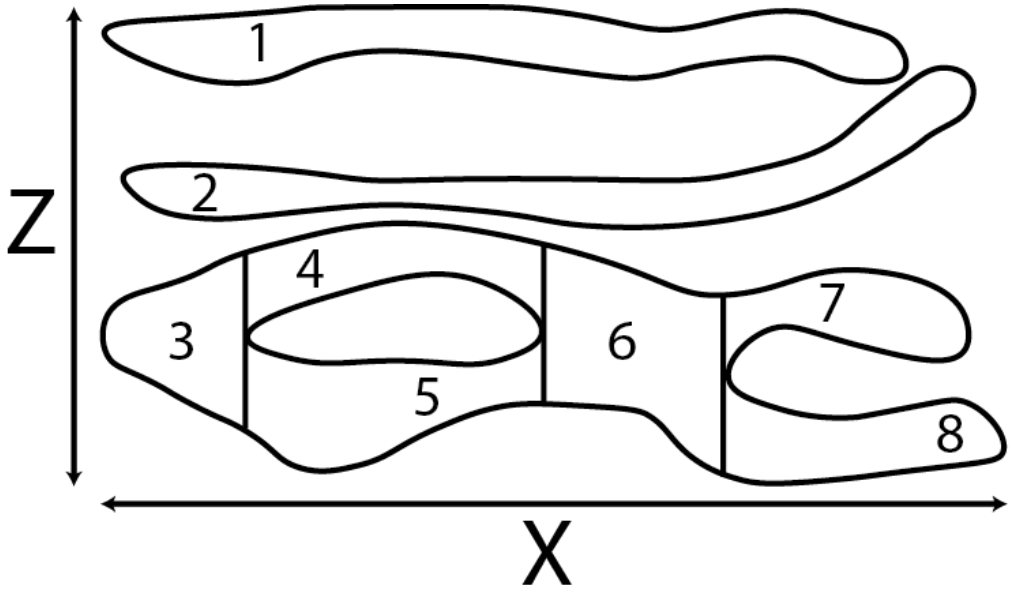

Figure 5 - Segmentation of Sound Scattering Layers (SSLs) features into individual SSLs. Each SSL was assigned a unique index value.

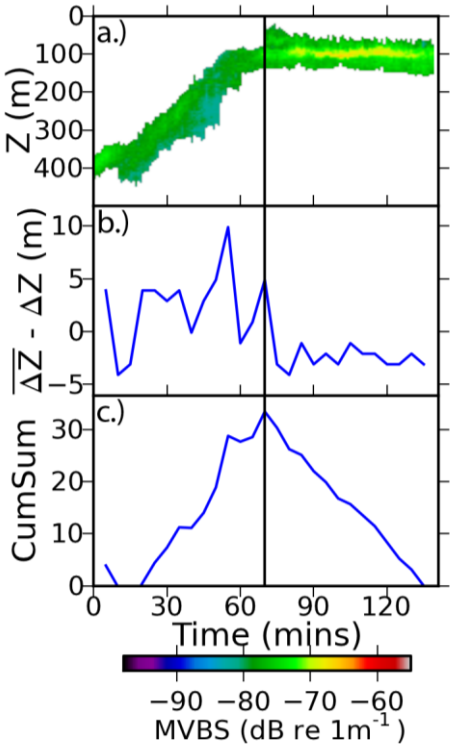

Figure 6 - Change Point Analysis of mean Sound Scattering Layer (SSL) depth – SSL taken from the example image in Fig. 4. The vertical black line at 70 minutes - the maximum point of the cumulative sum of b.) - indicates the point of separation of a static SSL and a migrant SSL. a.) SSL depth b.) The overall mean depth change of SSL minus each mean depth change in the time-series (binned at 6 min intervals) plotted in time c.) Cumulative sum of b: the maximum value indicates the most significant point of change.

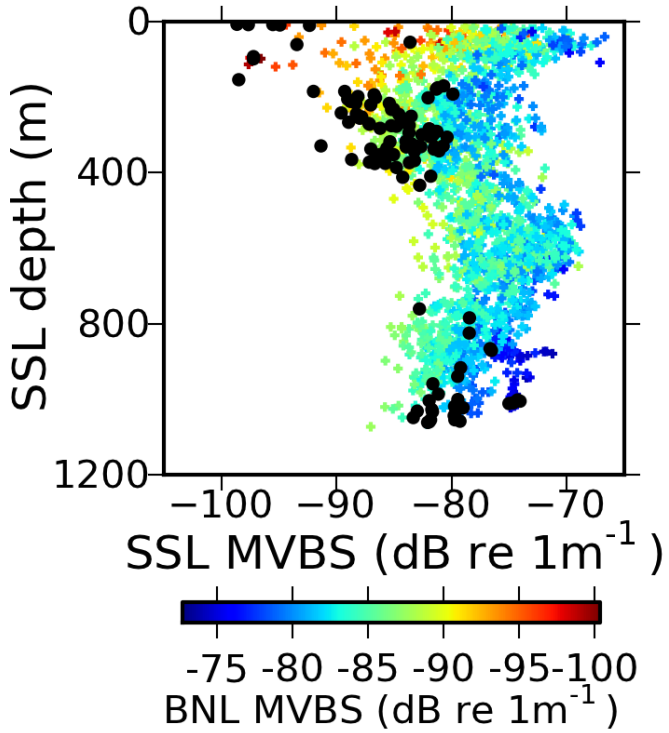

Figure 7 – Background Noise Level (BNL) for Sound Scattering Layers (SSLs) extracted from the IMOS dataset by SSL depth and MVBS. Black points represent phantom SSLs (incorrectly assigned SSLs) identified where BNL > SSL MVBS.

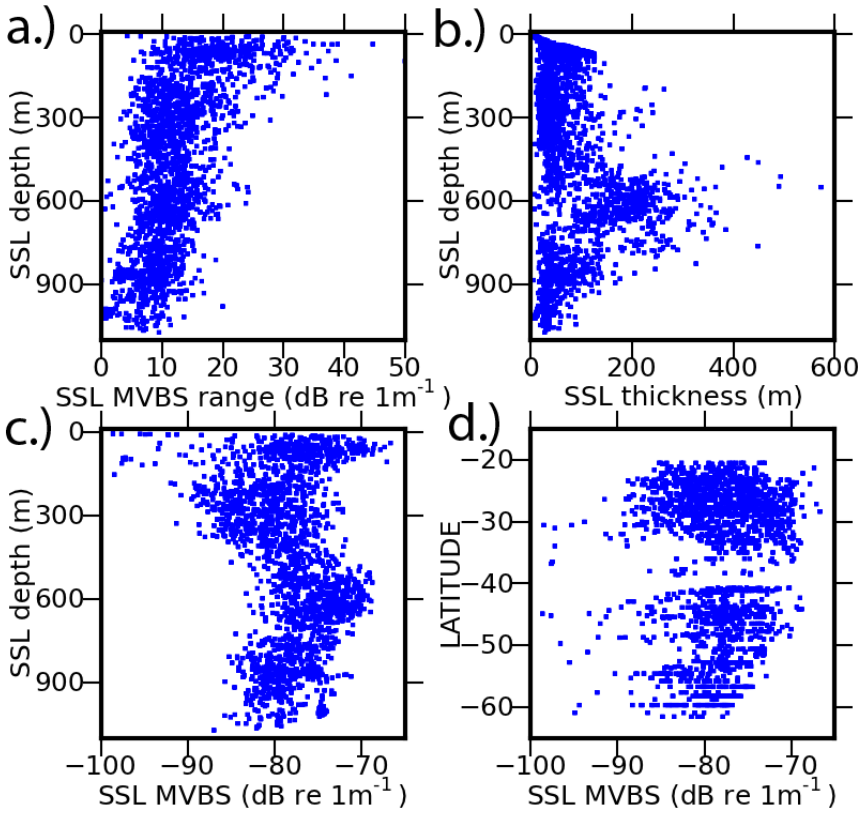

910

911 Figure 8 – Sound Scattering Layer (SSL) metrics extracted from the IMOS dataset. a.)

912 Water column heterogeneity: MVBS range serves as a proxy for biological complexity;

913 b.) SSL thickness as a function of depth; c.) Depth distribution of MVBS; d.) Latitudinal

914 distribution of MVBS.

915